NASA Technical Memorandum 105672

Application of Computational Fluid Dynamics to the Study of Vortex Flow Control for the Management of Inlet Distortion

Bernhard H. Anderson
Lewis Research Center
Cleveland, Ohio

and

James Gibb
Defense Research Agency
Bedford, England

Prepared for the
28th Joint Propulsion Conference and Exhibit
cosponsored by the AIAA, SAE, ASME, and ASEE
Nashville, Tennessee, July 6–8, 1992

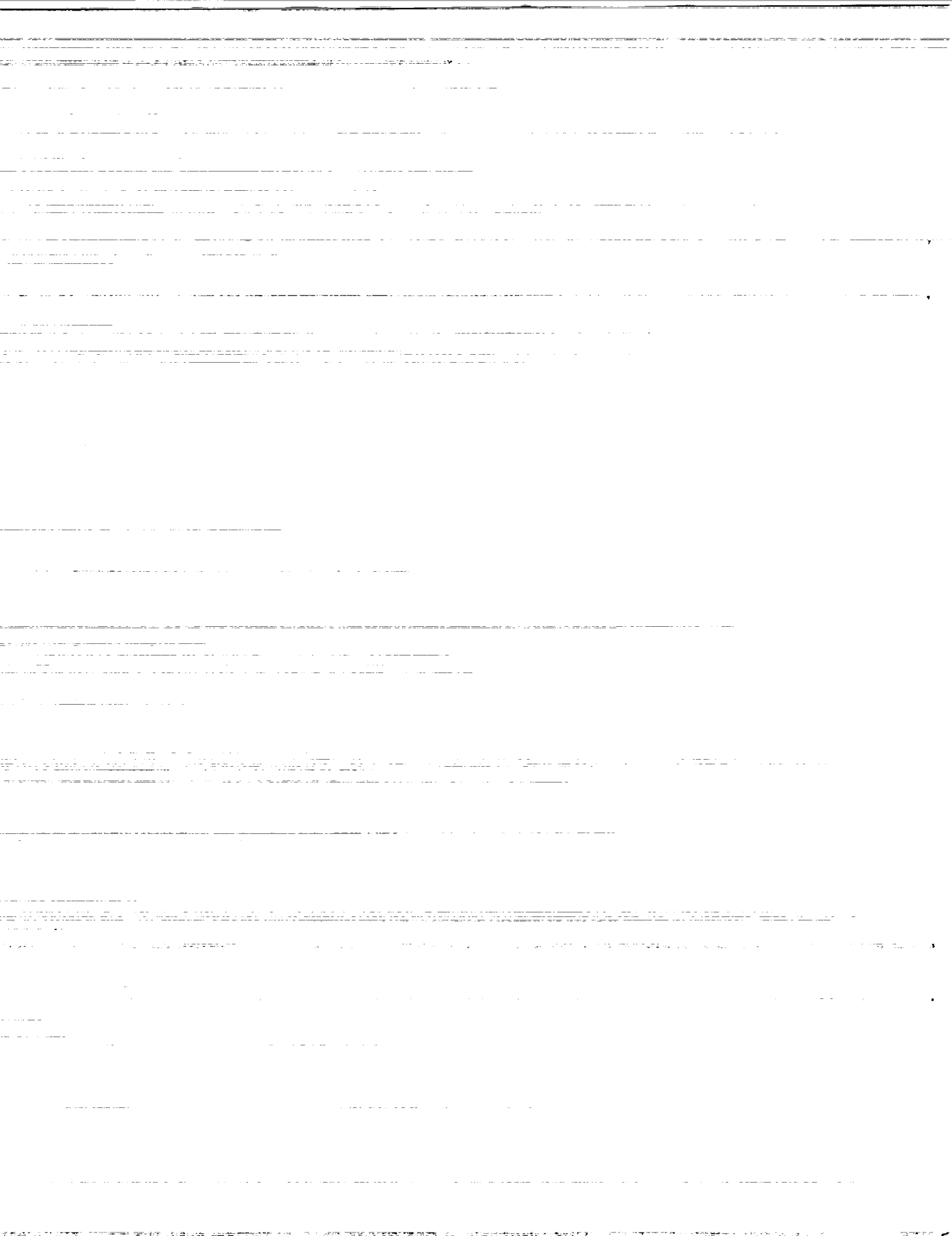

APPLICATION OF COMPUTATIONAL FLUID DYNAMICS TO THE STUDY OF VORTEX FLOW CONTROL FOR THE MANAGEMENT OF INLET DISTORTION

by

Bernhard H. Anderson
NASA Lewis Research Center
Cleveland, OH 44135

and

Dr. James Gibb
Defense Research Agency
Bedford, England

ABSTRACT

The present study demonstrates that the Reduced Navier Stokes code RNS3D can be used very effectively to develop a vortex generator installation for the purpose of minimizing the engine face circumferential distortion by controlling the development of secondary flow. The computing times required are small enough that studies such as this are feasible within an analysis-design environment with all its constraints of time and costs. This research study also established the nature of the performance improvements that can be realized with vortex flow control, and suggests a set of aerodynamic properties (called observations) that can be used to arrive at a successful vortex generator installation design. The ultimate aim of this research is to manage inlet distortion by controlling secondary flow through an arrangements of vortex generators configurations tailored to the specific aerodynamic characteristics of the inlet duct. This study also indicated that scaling between flight and typical wind tunnel test conditions is possible only within a very narrow range of generator configurations close to an optimum installation. This paper also suggests a possible law that can be used to scale generator blade height for experimental testing, but further research in this area is needed before it can be effectively applied to practical problems. Lastly, this study indicated that vortex generator installation design for inlet ducts is more complex than simply satisfying the the requirement of attached flow, it must satisfy the requirement of minimum engine face distortion.

NOMENCLATURE

A_i	=	inlet throat area
c	=	generator chord length
c_1	=	decay constant defined by Eq. (3)
C_f	=	wall skin friction coefficient
d	=	lateral spacing between generator blades
D_i	=	inlet throat diameter
DC_{60}	=	distortion descriptor defined as the maximum $(Pt_{ave} - Pt_{min})/Pt_{ave}$ in any 60.0° sector
h	=	generator blade height
L	=	length of inlet duct
M_i	=	inlet throat Mach number
n_{vg}	=	number of vortex generator pairs
Pt_0	=	free stream total pressure
Pt_{ave}	=	average total pressure at the engine face
Pt_{min}	=	minimum total pressure at engine face d10 in any sector of extent 60.0°
q_{ave}	=	average dynamic pressure at the engine face
r	=	distance between field point and generator tip
R_i	=	inlet throat radius
R_{ef}	=	engine face radius
Rey	=	inlet Reynolds number based on throat diameter
Tt_0	=	free stream total temperature
u	=	flow velocity at generator tip
X, Y, Z	=	primary cartesian coordinates
X_{cl}, Y_{cl}, Z_{cl}	=	cartesian coordinates along inlet centerline
X_{vg}	=	axial location of generator sector region
α	=	aerodynamic angle of incidence, radians
α_{vg}	=	generator spacing angle
β_{vg}	=	vane angle of incidence
δ	=	boundary layer thickness
ΔPt	=	total pressure loss of vortex generators
Γ_0	=	vortex strength at tip of generator, defined by Eq. (2)
Γ_r	=	vortex strength at field point in cross-section, defined by Eq. (1)
ρ	=	fluid density
θ_t	=	generator sector angle

INTRODUCTION

Modern tactical aircraft are required to be maneuverable at subsonic, transonic, and supersonic speeds, without giving up good cruise performance. Consequently, proper integration of the engine inlet with the airframe is of paramount importance. Regarding the enhancement of inlet performance and operation, design for optimum airframe-inlet integration has the following goals: (1) to minimize approach flow angularity with respect to the inlet cowl lip, (2) to deliver uniform, high pressure recovery flow to the inlet face, (3) to prevent or minimize vortex, wake, and boundary layer ingestion by the inlet throughout the flight envelope, (4) to reduce FOD/hot gas ingestion by the inlet, and finally (5) to minimize the potential for flow field interference from weapon carriage/firing, landing gear deployment, tanks, pods, or other hardware. The combination of inlet design and airframe integration must not only provide high pressure recovery to maintain the desired thrust levels, but also generate low flow distortion consistent with stable engine operation.

Engine face flow distortion is one of the most troublesome and least understood problems for designers of modern inlet engine systems.[1-2] One issue is that there are numerous sources of flow field distortion that are ingested by the inlet or generated within the inlet duct itself. Among these sources are (1) flow separation at the cowl lip during maneuvering flight, (2) flow separation on the compression surfaces due to shock-wave boundary layer interactions, (3) spillage of the fuselage boundary layer into the inlet duct, (4) ingestion of aircraft vortices and wakes emanating from upstream disturbances, and (5) secondary flow and possibly flow separation within the inlet duct itself. Most aircraft have experienced one or more of these types of problems during development, particularly at high Mach numbers and/or extreme maneuver conditions, such that flow distortion at the engine face exceeded allowable surge limits. Such compatibility problems were encountered in the early versions of the B70, the F-111, the F-14, the MIG-25, the Tornado and the Airbus A300 to name a few examples.

One of the most commonly used methods to control local boundary layer separation within diffusing ducts is the placement of vortex generators upstream of the problem area. Vortex generators in use today are small wing sections mounted on the inside surface of the inlet inclined at an angle to the on-coming flow to generate a shed vortex. The generators are usually sized to the local boundary layer height for the best interaction between the shed vortex and boundary layer, and are usually placed in groups of two or more upstream of the problem area. The principle of boundary layer control using vortex generators in this manner relies on induced mixing between the external or core stream and the boundary layer.

It was not until the confirmation test by Kaldschmidt Syltebo, and Ting,[3] on the 727 center inlet for the refanned JT8D engine that an attempt was made to use vortex generators to restructure the development of secondary flow in order to improve the engine face distortion level. With this work, a very important shift in strategy on the use of vortex generators had occurred. The perspective had moved from a local one, in which the goal was to prevent boundary layer separation, to a global one, in which the goal was to manage secondary flow in order to minimize engine face distortion. However, in order to effectively accomplish this new goal, the design strategy must shift from an experimental to an analysis based methodology, because of the high costs associated with experimental parametric studies.

The overall objective of this study is to advance the understanding, the prediction, and the control of inlet distortion, and to study the basic interactions that are involved in the management of secondary flows within inlet ducts using Computational Fluid Dynamics. To this end, a series of observations were made by Anderson, Huang, Paschal, and Cavatorta,[4] concerning the importance of various vortex generator design parameters in minimizing engine face distortion within the 727/TAY651-54 center inlet S-duct. This paper continues with an examination of the central question as to whether judgements about generator installations optimized for flight conditions can be drawn from scaled wind tunnel test results, and enlarges on the study of the aerodynamic properties of engine face distortion and its control to cover a wider range of flow conditions. Specifically, the goals of the present paper are: (1) to demonstrate the capability of the Reduced Navier Stokes code RNS3D to design a vortex generator system for the RAE2129 inlet S-duct, which will be tested over a wide range conditions including angle-of-incidence and angle-of-yaw, (2) to investigate the similarities and differences between designing and testing generator installations under flight and scaled wind tunnel test conditions, and (3) to make some formal observations concerning the importance of various vortex generator installation parameters in minimizing engine face distortion over a range of flow conditions from typical scaled wind tunnel test to flight Reynolds numbers.

THEORETICAL BACKGROUND

Three dimensional viscous subsonic flows in complex inlet duct geometries are investigated by a numerical procedure which allows solution by spatial forward marching integration, utilizing flow approximations from the velocity-decomposition approach of Briley and McDonald.[5-6] The goal of this approach is to achieve a level of approximation that will yield accurate flow predictions, while reducing the labor below that needed to solve the full Navier Stokes equations. The governing equations for this approach have been given previously for orthogonal coordinates, and the approach has been applied successfully to problems whose geometries can be fitted conveniently with orthogonal coordinate systems. However, geometries encountered in typical subsonic inlet ducts cannot be treated easily using orthogonal coordinates, and this led to an extension of this approach by Levy, Briley, and McDonald,[7] to treat ducted geometries with nonorthogonal coordinates. In generalizing the geometry formulation, Anderson,[8] extended the analysis to cover ducted geometries defined by an externally generated gridfile, such that it allowed for (1) reclustering the existing gridfile, (2) redefining the centerline space curve, and (3) altering the cross-sectional shape and area distribution without returning to the original gridfile. This version of the 3D RNS computer code is called RNS3D.

Vortex Generator Model

The model for the vortex generators within the RNS analysis takes advantage of the stream function-vorticity formulation of the governing equations. The shed vortex is modeled by introducing a source term into the vorticity equation that is a function of the geometric characteristics of the generators themselves. This source term is introduced at every point in the cross-plane in the form of the following expression

$$\Gamma_p = \Gamma_0 e^{-(c_1 r^2)} \tag{1}$$

where Γ_p is the vortex strength at any point in the cross-plane, Γ_0 is the vortex strength at the tip of the generator, r is the distance between the field point and the tip of the generator, and c_1 is a constant which controls the decay of the shed vortex strength in the cross-plane. The geometry of the generator is related to the vortex strength at the blade tip through the term Γ_0, defined by

$$\Gamma_0 = 8.0 \rho u c \tanh(\alpha) \tag{2}$$

where ρ is the fluid density, u is the velocity of the flow at the generator tip, c is the chord length, and α is the aerodynamic angle of attack in radians. The decay constant c_1 in Eq. (1) is given by the expression

$$c_1 = 4.0/c^2 \tag{3}$$

This vortex model resembles the one proposed by Squire,[9] except that it neglects the variation of viscosity in the cross-plane. Although there is limited experimental data in the literature to validate computer codes for the analysis of installed vortex generator systems, RNS3D and the generator model described by Eqs. (1) through (3), have been validated for three (3) pairs of counter-rotating vortex generators installed in the University of Tennessee diffusing S-duct,[10] and verified for an installation composed of nine (9) pairs of co-rotating generators and seven (7) pairs of counter-rotationg generators within the 727/TAY651-54 center inlet,[4] all with very good results.

RESULTS AND DISCUSSIONS

Vortex Generator Design Considerations

An extensive study was undertaken to develop a vortex generator installation for the RAE2129 inlet S-duct, and to examine the the relationship between the important design variables for the purpose of developing an understanding on how best to control inlet distortion. It was established[4] that vortex generator design for the purpose of minimizing engine face distortion depends on the initial conditions, i.e. generator installation design is a point design and all other flow conditions are off-design. Thus the installed performance achieved over a range of conditions depends on compromises made in the geometry, arrangement, and location of the vortex generators within the inlet duct. For that reason, this paper will consider four generator installation designs each based on different objectives. The four generator designs include; (1) an optimum vortex generator installation designed for the AGARD Test Case 3.2

flow conditions, (2) an optimum vortex generator configuration designed for the AGARD Test Case 3.1 flow conditions, (3) a vortex generator installation optimized for flight conditions, and (4) a generator installation with the same geometry as that optimized for flight conditions, but relocated within the inlet to operate at the Test Case 3.2 initial conditions. The purpose of the last two generator configurations is to determine whether judgements about generator configurations optimized for flight conditions can be drawn from scaled wind tunnel tests results. The AGARD Test Cases 3.1 and 3.2 are considered to be of typical scaled wind tunnel test results, and are defined by:

AGARD Case 3.1 Test and Initial Conditions

Total Pressure	$Pt_0 = 29.889\ in.\ Hg$
Total Temperature	$Tt_0 = 293°\ K$
Throat Mach Number	$M_t = 0.794$
Throat Diameter	$D_t = 5.071\ in.$
Throat Area	$A_t = 25.254\ in.^2$
Reynolds Number (based on D_t)	$Rey = 1.848x10^6$

AGARD Case 3.2 Test and Initial Conditions

Total Pressure	$Pt_0 = 29.865\ in.\ Hg$
Total Temperature	$Tt_0 = 293°\ K$
Throat Mach Number	$M_t = 0.412$
Throat Diameter	$D_t = 5.071\ in.$
Throat Area	$A_t = 25.254\ in.^2$
Reynolds Number (based on D_t)	$Rey = 1.158x10^6$

Flight conditions for this study are considered to be a throat Mach number M_t of 0.412 and Reynolds number Rey of $8.264x10^6$ based on inlet throat diameter.

Installed Vortex Generator Performance Characteristics

The RAE2129 inlet duct geometry and computational mesh used in this study is shown in Fig. 1, and was based on a study by Willmer, Brown, and Goldsmith.[11] The centerline of the inlet defined in terms of the coordinate system shown in Fig. 1 is given by:

$$Z_{cl} = -\Delta Z_{cl}\left[1 - \cos\left(\pi \frac{X_{cl}}{L}\right)\right] \qquad (4)$$

where X_{cl} is the x-coordinate of the inlet duct centerline, and ΔZ_{cl} in the centerline offset. The radius distribution measured perpendicular to the duct centerline is given by:

$$\left(\frac{R - R_i}{R_{ef} - R_i}\right) = 3\left(1 - \frac{X_{cl}}{L}\right)^4 - 4\left(1 - \frac{X_{cl}}{L}\right)^3 + 1 \qquad (5)$$

where R_i is the inlet throat radius, R_{ef} is the engine face radius, and L is the length of the inlet. For the purposes of the calculations, the RAE2129 S-duct was nondimensionalized with respect to the throat radius, thus $R_i = 1.0$, $R_{ef} = 1.183$, $L = 7.10$, and $\Delta Z_{cl} = 2.13$.

A polar grid topology was chosen for the RAE2129 S-duct which consisted of 49 radial, 49 circumferential, and 121 streamwise nodal points in the half plane, for a total number of 290,521 grid points. The CPU time was 8.3 minutes on the CRAY XMP for this computational grid. The large number of mesh points was chosen in order to resolve the small interactions that are characteristic of vortex generator flow fields within the inlet duct. The internal grid was constructed such that the transverse computational plane was perpendicular to the duct centerline. Grid clustering was used in the radial direction in order to redistribute the nodal points to resolve the high shear regions near the wall. The flow in the inlet was considered turbulent throughout. The inflow boundary layer condition corresponds to a shear layer thickness $\delta/R_i = 0.120$, and were applied one diameter upstream of the inlet entrance in the constant area extension.

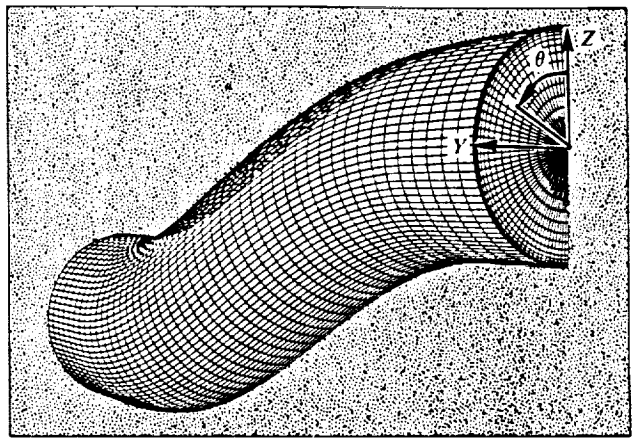

Fig. (1) - Geometry definition for the RAE2129 intake duct.

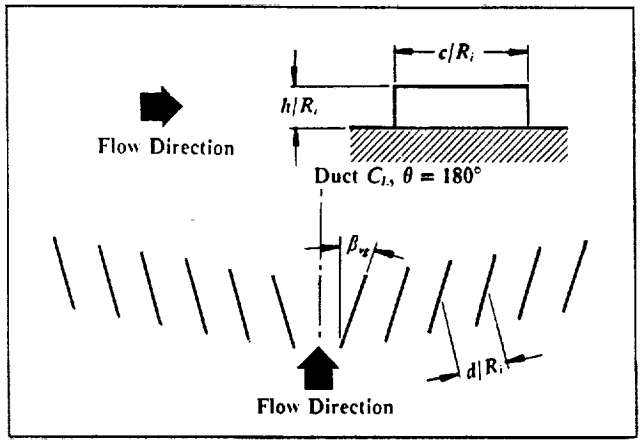

Fig. (2) - Geometry definition of co-rotating vortex generators.

The geometry of the co-rotating vortex generators used in this study along with the nomenclature used in positioning the individual blades are presented in Figs. 2 and 3. The important geometric design parameters include: (1) the vortex generator blade height h/R_i, (2) the blade chord length c/R_i, and (3) the vane angle of attack β_{vg}. Instead of the usual spacing parameter d/R_i, i.e. the distance between adjacent blades, the positioning of the vortex generator blades was described in terms of a lateral spacing angle α_{vg} and a sector angle over which the blades were positioned θ_s. For this study, the relationship between blade spacing angle α_{vg} and sector angle θ_s is given by

$$\theta_s = \alpha_{vg}\left(n_{vg} - \frac{1}{2}\right) \qquad (6)$$

where n_{vg} is the number of pairs of vortex generator blades. Eq. (6) was also used to position the individual generator blades around the inside periphery of the inlet duct at a given axial sector location X_{vg}/R_i. The angle θ_s was measured counter-clockwise relative to an azimuthal angle of 180° with respect to the vertical axis of the duct. It should be remembered that only a half-duct calculation was performed in this study, and Eq. (6) is used to place the individual vortex generators within that half-duct. Thus, the total number of vortex generators within the real inlet is twice the number actually used in the calculation. Also, since the other half of the inlet duct is the mirror image of the computational duct, each co-rotating generator can be view as having a corresponding mirror image, i.e. the co-rotating vortex generators can be labeled as pairs. Shown in Fig. 4 are the axial locations of the vortex generator sector regions

covered in this study. These sector regions were positioned between $X_{vg}/R_i = 1.0$ and $X_{vg}/R_i = 5.0$ and covered a sector angle θ_s up to 157.5° in half-plane computational duct, or 315.0° in the real duct.

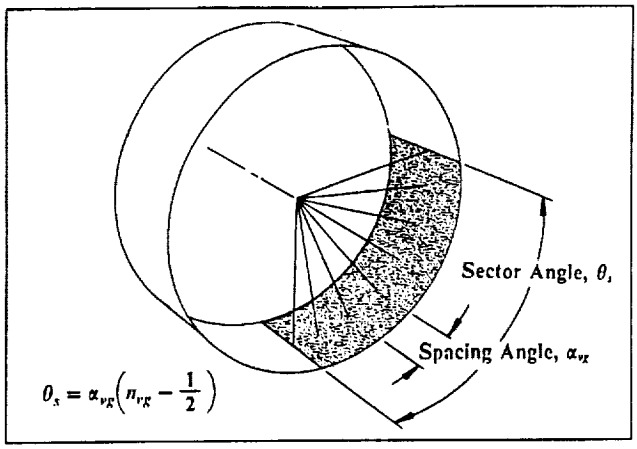

Fig. (3) - Nomenclature used for vortex generator positioning.

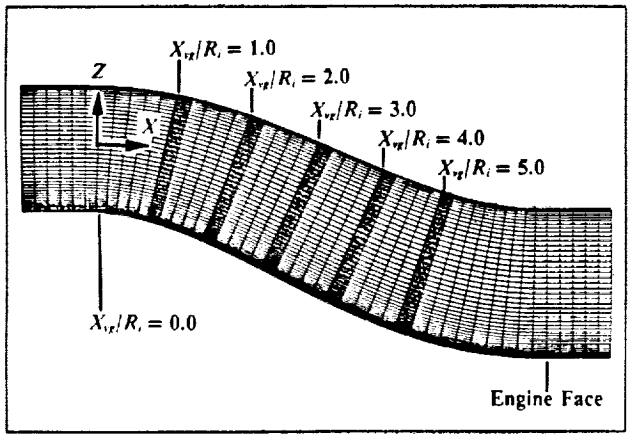

Fig. (4) - Axial locations of the vortex generator sector regions.

The standard blade section used in this study was composed of a low aspect ratio flat-plate vane type generator, where the ratio of blade height to chord length h/c was fixed at 0.259, and the vane angle-of-incidence β_{vg} was set at 16.0°. Although not part of this study, it has been found that the strength of the individual vortex from the generator blade does not vary rapidly with vane angle-of-incidence β_{vg} for low aspect ratio vanes, and so the system is relatively insensitive to changes in local flow direction on the surface. This is in agreement with the conclusions reached by Pearcy[12] who obtained his information from experimental measurements.

For comparison with the experimentally measured inlet performance, computation were made at inlet throat Mach numbers of 0.794 and, and 0.412, and corresponding Reynolds numbers of $1.848x10^6$ and $1.158x10^6$ based on inlet throat diameter D_i. These correspond to the AGARD Test Case 3.1 and 3.2 initial conditions previously defined. Figs. 5 and 6 show a comparision between the measured and calculated engine face total pressure recovery and engine face DC_{60} distortion for the RAE2129 S-duct inlet without vortex flow control and with vortex generator configuration VG130 installed in the inlet. Vortex generator installation VG130, which is the configuration optimized for the Test Case. 3.2 initial flow conditions, gave the best overall performance between Mach numbers 0.10 to 0.80, and is defined by:

Vortex Generator Configuration VG130

Number of Co-Rotating Generator Pairs:	$n_{vg} = 11$
Vortex Generator Sector Location:	$X_{vg}/R_i = 3.0$
Generator Blade Height:	$h/R_i = 0.075$
Generator Chord Length:	$c/R_i = 0.2896$
Generator Spacing Angle:	$\alpha_{vg} = 15.0°$
Generator Vane Angle-of-Attack:	$\beta_{vg} = 16.0°$
Generator Sector Angle:	$\theta_s = 157.5°$

The theoretical performance is shown in Figs. 5 and 6 as a function of inlet throat Mach number, at Reynolds number corresponding to the Test Case 3.1 and Test Case 3.2 initial conditions, i.e. $Rey = 1.848x10^6$ and $Rey = 1.158x10^6$ respectively. For the range of inlet throat Mach numbers between 0.412 and 0.794, the analysis indicated the flow separated, and the separation was that associated with vortex lift-off.[10] The separation (or vortex liftoff) occurring at an inlet Mach number of 0.412 was "weak", and progressively increased in strength as the throat Mach number increased, becoming quite severe at an inlet Mach number of 0.794. RNS3D was able to predict the total pressure recovery for "weak" separation quite well, but the difference between analysis and measurements become progressively worse as the separation increases in strength, i.e. as its influence on the overall inlet flow field becomes more pronounced. The over prediction of inlet total pressure recovery at the higher throat Mach numbers results from the fact that current turbulence models are unable to represent severe turbulent separation (or vortex lift-off) with sufficient accuracy to predict the separation location and total pressure losses. Current turbulence models invariably predict separation further downstream in the inlet duct than is indicated by measurements. The good predictions of the DC_{60} engine face distortion in the higher Mach number range probably resulted from compensating errors, although differences between calculations and measurements could also have occurred because the distortion parameter was evaluated from the computational mesh rather than the location of the probes on the measuring rake and the data reduction technique used in the experiment.

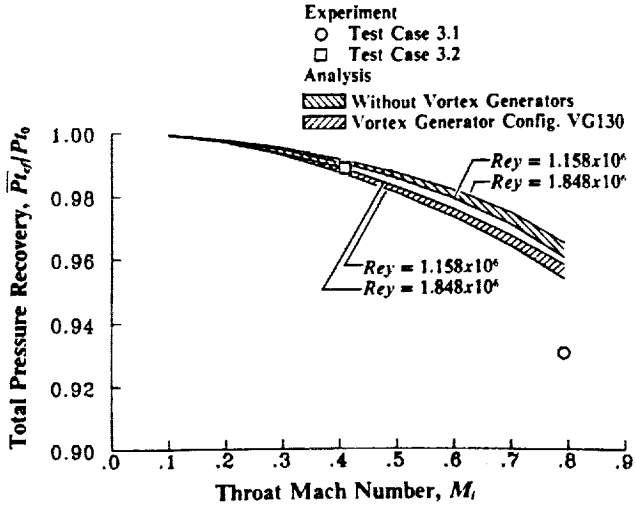

Fig. (5) - Effect of vortex flow control on engine face total pressure recovery for the RAE2129 intake duct, vortex generator configuration VG130.

With vortex generator configuration VG130 installed in the inlet, the flow remains attached over the entire Mach number range considered, affecting a number of important flow properties. First and foremost, vortex generator configuration VG130 suppressed both the Mach number and Reynolds number influence on the DC_{60} engine face distortion characteristics. Secondly, the level of engine face

circumferential distortion was reduced to a very acceptable level over a wide range of inlet throat Mach numbers. Thirdly, as a consequence of the vortex generator installation, an additional total pressure loss occurred as result of mixing between the vortex flow and the main flow within the inlet. Theses losses are a function of both Mach number and Reynolds number.

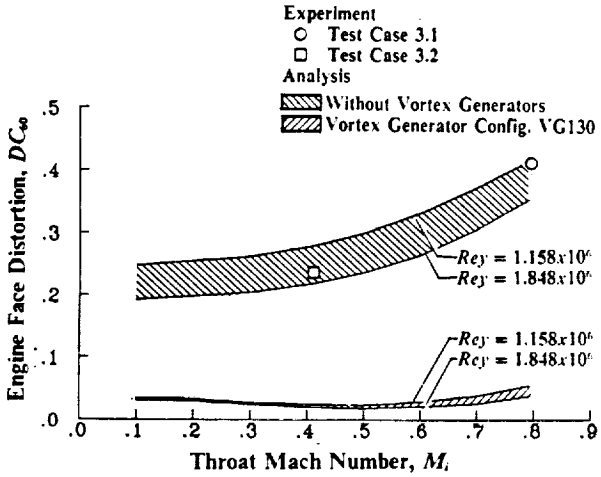

Fig. (6) - Effect of vortex flow control on engine face DC_{60} distortion for the RAE2129 intake duct, vortex generator configuration VG130.

Along a constant Reynolds number line, the strength of the secondary flow decreased as the throat Mach number or weight flow decreased, and this resulted in a rapid lowering of the engine face distortion in the Mach number range between 0.794 and 0.412. In the Mach number range between 0.412 and 0.10, where the flow remains attached to the inlet walls, the DC_{60} distortion decreased more slowly, becoming almost constant, and approaching a finite value at zero Mach number (see discussion below). This results from the fact that the secondary flow decreased at about the same rate as the average engine face dynamic pressure. However, the combined interaction between the induced secondary flow and vortex flow established by the generator installation was such that the resultant secondary flow always decreased at about the same rate as the average engine face dynamic pressure. This combined interaction resulted in an 'essentially constant' DC_{60} engine face distortion over the entire inlet throat Mach number range from 0.10 to 0.794, and a suppression of the Reynolds number influence between $Rey = 1.158x10^6$, and $Rey = 1.848x10^6$. It should be indicated here that the installed characteristics of vortex generator configuration VG130 resulted from proper sizing and arrangement of the generator blades, as well as location with the inlet duct. Had another size, arrangement or location of generators been chosen, the installed results could be very different.

It is important to indicate that the DC_{60} distortion descriptor has the interesting property that both the numerator (defined by the pressure difference $Pt_{av} - Pt_{min}$) and the denominator (defined by the average dynamic pressure q_{av} at the engine face) approach zero as the inlet throat Mach number approaches zero. In addition, in examining inlet throat Mach number effects on DC_{60} engine face distortion, it is important to understand that what is being measured is the change in a pressure difference relative to the the average engine face dynamic pressure, both of which decrease with Mach number. The pressure difference $Pt_{av} - Pt_{min}$ is affected by inlet throat Mach number in two ways, namely (1) as a simple compressibility effect, and (2) as changes in the strength and development secondary flow itself. It is the changes in the strength and development of secondary flow over the flight envelope that is the very heart of understanding inlet distortion.

Generator Influence on Engine Face Flow Field

Presented in Figs. 7 through 10 are the engine face total pressure recovery maps and secondary flow field without vortex generators and with vortex generator configuration VG130 installed in the RAE2129 inlet duct, for both Test Case 3.1 and 3.2 initial conditions. Also shown on these figures are the DC_{60} engine face distortion values, and the engine face total pressure recovery $\overline{Pt_{ef}}/Pt_0$ values. The performance parameters $\overline{Pt_{ef}}/Pt_0$ and DC_{60} were computed using area weighted values from the computational mesh, rather than the rake used in the experiment.

It is evident from these figures that vortex generator configuration VG130 had the effect of distributing the low energy flow in a more uniform manner around the inside periphery of the engine face, thus decreasing the DC_{60} engine face distortion substantially. However, the penalty associated with this redistribution proccess is a decrease in engine face total pressure recover $\overline{Pt_{ef}}/Pt_0$. The computed total pressure loss $\Delta Pt/Pt_0$ associated with an installation composed of eleven (11) generator pairs is 0.008 at the Test Case 3.1 initial conditions and 0.004 at the Test Case 3.2 inlet conditions (see section entitled A Perspective on Vortex Generator Design for a discussion on the measured losses associated with generator installations at flight Reynolds numbers). Although mixing takes place between the high energy core flow and low energy boundary layer flow the primary gains result as a consequence of this redistribution process. Thus, vortex flow control of inlet distortion can also be viewed as creating a new secondary flow field that will redistribute the low energy flow in a more uniform manner at the engine face station.

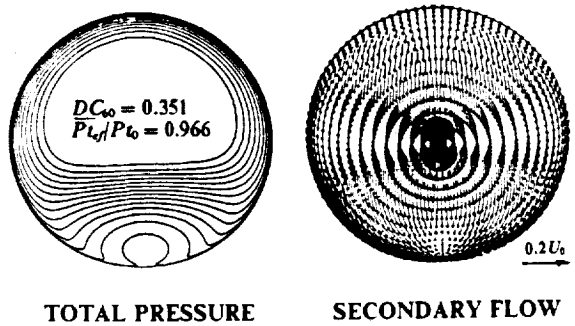

Fig. (7) - Engine face flow field for the RAE2129 intake duct without vortex generators, Test Case 3.1 initial conditions.

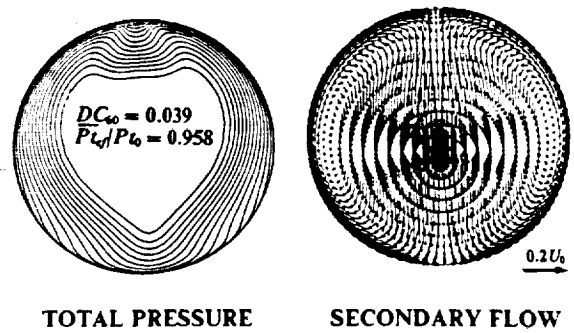

Fig. (8) - Engine face flow field for the RAE2129 intake duct with vortex generator configuration VG130, Test Case 3.1 initial conditions.

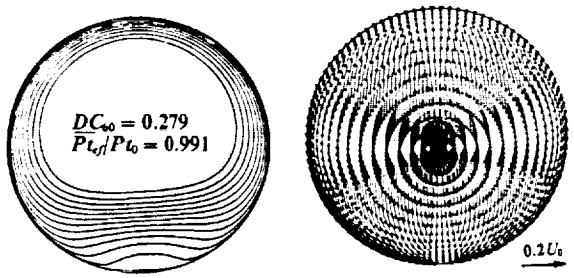

Fig. (9) - Engine face flow field for the RAE2129 intake duct without vortex generators, Test Case 3.2 initial conditions.

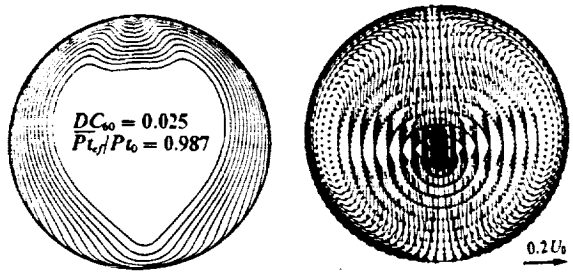

Fig. (10) - Engine face flow field for the RAE2129 intake duct with vortex generator configuration VG130, Test Case 3.2 initial conditions.

On the Differences Between Flight and Test Performance

Presented in Fig. 11 is the effect of vortex generator blade height h/R_i on engine face DC_{60} distortion at three inlet initial conditions, i.e. flight, Test Case 3.2, and Test Case 3.1 initial conditions. The vortex generator installation was composed of eleven (11) pairs of co-rotating generators located at an axial position $X_{vg}/R_i = 3.0$ with an angular lateral spacing α_{vg} of 15.0° between the generator blades. The results presented in Fig. 11 illustrate one of the primary differences between generator installations designed for flight conditions and those which are optimized for wind tunnel test conditions, i.e. the optimum blade height is smaller at the higher Reynolds numbers that are associated with flight conditions. Comparing the Test Case 3.2 and 3.1 performance results on Fig. 11 indicates Mach number M_i also plays a role in determining the optimum blade height. Figure 11 indicates the important characteristic that the installed performance degrades much faster at scaled test conditions than at flight conditions, hence the choice of blade height becomes a more critical decision at wind tunnel conditions. In summary, it can be observed from Fig. 11 that

For a given configuration of vortex generators positioned at a fixed axial location, there exists a blade height which will minimize the engine face distortion.

Figure 12 shows the effect vortex generator sector location X_{vg}/R_i on engine face DC_{60} distortion at the three initial conditions and corresponding optimum generator blade height h/R_i determined from Fig. 11. The generator installation was again composed of eleven (11) co-rotating blades using an angular spacing α_{vg} of 15.0°. These optimum generator blade heights h/R_i were determined to be 0.060 for flight conditions, 0.075 for the AGARD Test Case 3.2 condition, and 0.080 for the AGARD Test case 3.1 initial conditions. At each of these optimum generator blade heights and test conditions, the location for these installations were all at the same axial location at $X_{vg} = 3.0$. Figure 12 also demonstrates that scaling between flight and wind tunnel test conditions are possible only in the neighborhood of a vortex generator installation that has been optimized for blade height and sector location, i.e. an optimum generator design. The numerical results of this paper suggests that a Mach number and Reynolds number expression for optimum generator blade height of the form:

$$h = k(M_i)Rey^{-0.118} \tag{7}$$

may be applicable to scale an installation design for flight so that it can be tested under wind tunnel conditions, although the generator installation under study must be close to an optimum configuration. However, the total pressure recovery $\overline{Pt_{e_f}}/Pt_0$ will not scale since it is a function of Reynolds number, and the off-design characteristics such as angle-of-incidence and angle-of-yaw will probably scale only within the neighborhood of the conditions used to optimize the generator installation. Figure 12 also indicates that the degradation in performance as the flow conditions move further from that which were used to optimize the vortex generator installation is much faster under test conditions that at flight conditions. This characteristic can be related to the generator scale effect δ/h (ratio of boundary layer thickness to generator blade height) and is caused by the fact that in three dimensional inlet ducts, the boundary layer thickness changes more rapidly at the lower Reynolds numbers as a result of the effects of secondary flow. Because of this characteristic, the placement of the generator is more critical at tunnel test conditions than it is at flight conditions, but the following fundamental aerodynamic property is still a valid observation over a wide range of flow conditions:

For a given geometry and arrangement of vortex generators, there exists an axial location which will minimize engine face distortion at a given inlet flow condition.

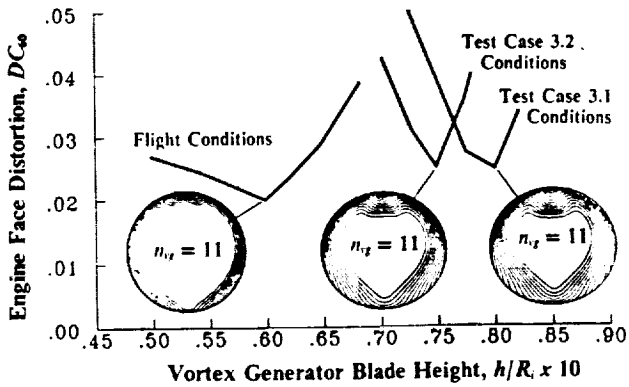

Fig. (11) - Effect of vortex generator blade height (h/R_i) on engine face DC_{60} distortion at three inlet initial conditions.

The results indicated in Figs. 11 and 12 defined three vortex generator installations, namely (1) an optimum vortex generator installation designed for the AGARD Test Case 3.2 flow conditions, (2) an optimum vortex generator configuration designed for the AGARD Test Case 3.1 flow conditions, (3) a vortex generator installation optimized for flight conditions. These generator configurations have been labeled VG130, VG230, and VG430 respectively. Vortex generator installation VG130 has been previously defined, however, configuration VG230 and VG430 are specifically defined as:

Vortex Generator Configuration VG230

Number of Co-Rotating Generator Pairs:	$n_{vg} = 11$
Vortex Generator Sector Location:	$X_{vg}/R_i = 3.0$
Generator Blade Height:	$h/R_i = 0.080$
Generator Chord Length:	$c/R_i = 0.2896$
Generator Spacing Angle:	$\alpha_{vg} = 15.0°$
Generator Vane Angle-of-Attack:	$\beta_{vg} = 16.0°$
Generator Sector Angle:	$\theta_s = 157.5°$

Vortex Generator Configuration VG430

Number of Co-Rotating Generator Pairs:	$n_{vg} = 11$
Vortex Generator Sector Location:	$X_{vg}/R_i = 3.0$
Generator Blade Height:	$h/R_i = 0.060$
Generator Chord Length:	$c/R_i = 0.2896$
Generator Spacing Angle:	$\alpha_{vg} = 15.0°$
Generator Vane Angle-of-Attack:	$\beta_{vg} = 16.0°$
Generator Sector Angle:	$\theta_s = 157.5°$

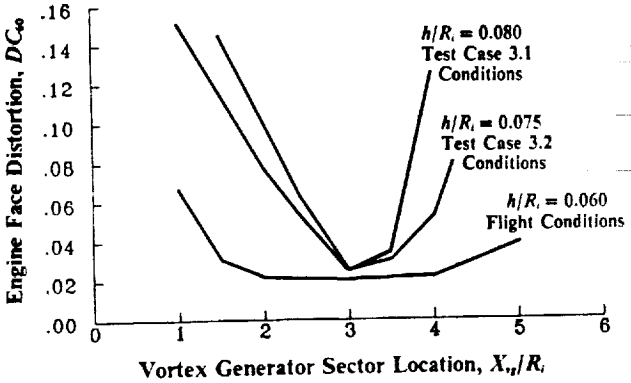

Fig. (12) - Effect of vortex generator sector location (X_{vg}/R_i) on engine face DC_{60} distortion at three inlet initial conditions and corresponding optimum generator blade heights (h/R_i).

It is apparent from the discussions of Figs. 11 and 12 that the generator scale δ/h (i.e. the ratio of local boundary layer thickness to generator blade height) plays a very important role in determining installed vortex generator performance and also suggests that a generator installation optimized for flight can be relocated within the inlet to give the similar performance as in scaled wind tunnel tests. Figure 13 presents the effect of generator sector location X_{vg}/R_i on engine face DC_{60} distortion for generator configuration VG430 operating both at Test Case 3.2 and flight conditions. At flight conditions, the optimum axial position for configuration VG430 is at a location $X_{vg}/R_i = 3.0$, and this location provides very low engine face distortion. However, the distortion of this generator configuration at the Test Case 3.2 conditions is very high. By moving the VG430 configuration forward where the boundary layer is thinner, the engine face DC_{60} distortion decreases to a more acceptable level. This defines the fourth generator installation in this series, i.e. (4) a generator installation with the same geometry as that optimized for flight conditions, but relocated within the inlet to operate at the Test Case 3.2 initial conditions. This configuration of co-rotating vortex generators is defined as:

Vortex Generator Configuration VG310

Number of Co-Rotating Generator Pairs:	$n_{vg} = 11$
Vortex Generator Sector Location:	$X_{vg}/R_i = 1.0$
Generator Blade Height:	$h/R_i = 0.060$
Generator Chord Length:	$c/R_i = 0.2896$
Generator Spacing Angle:	$\alpha_{vg} = 15.0°$
Generator Vane Angle-of-Attack:	$\beta_{vg} = 16.0°$
Generator Sector Angle:	$\theta_s = 157.5°$

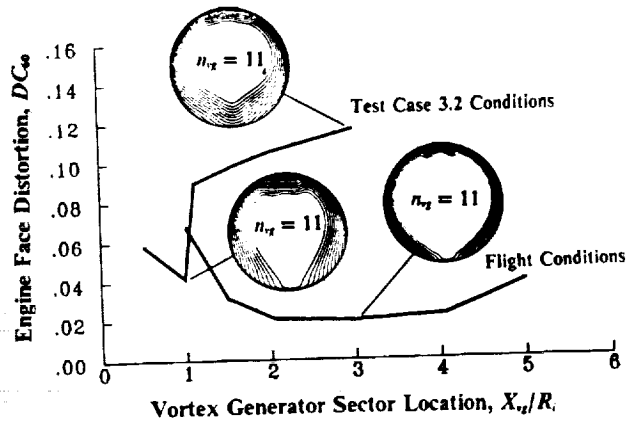

Fig. (13) - Effect of vortex generator sector location (X_{vg}/R_i) on engine face DC_{60} distortion, vortex generator configuration VG430, Test Case 3.2 and flight conditions.

Figure 14 presents the effect of vortex generator sector location X_{vg}/R_i on the engine face DC_{60} distortion with vortex generator configuration VG430 (defined above) at flight conditions. The total pressure recovery maps shown in Fig. 14 indicates the manner in which the performance changes with axial position and suggests that this generator installation increases in strength as its location is moved upstream from the optimum postion and decreases in strength as the generator installation is moved downstream relative to this optimum location. Under angle-of-incidence or angle-of-yaw conditions, it would be expected that the overall ratio of boundary layer thickness to generator height δ/h to increase, and therefore a decrease in the overall effectiveness of the generator installation can be expected. However, by moving the generator installation forward of its optimum position, the overall performance at angle-of-incidence and angle-of-yaw can be improved and even optimized, i.e. the aerodynamic properties of vortex flow control that have been discussed are valid at the off-design conditions of angle-of-incidence and angle-of-yaw.

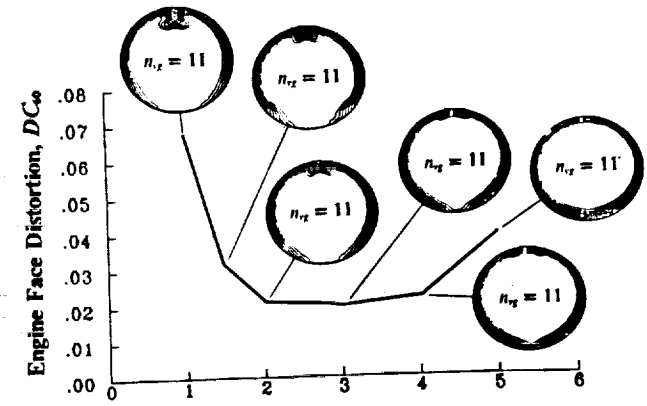

Fig. (14) - Effect of vortex generator sector location (X_{vg}/R_i) on engine face DC_{60} distortion, vortex generator configuration VG430, flight conditions.

Observations on Vortex Generator Installation Design

The relative engine face distortion levels at different flight conditions is important since inlets must be designed to operate with low distortion over a flight envelope. Trades between what is needed at one flight condition, such as takeoff, and what is needed at other conditions, such as transonic maneuvering at low altitudes or cruise, must be made. Reynolds number, Mach number, inlet mass flow

and engine tolerance can all change from one operating condition to another. It is important therefore to understand the influence of these various operating factors as well as the large number of design parameters associated with the geometry, arrangement, and placement of the generators within the inlet duct. One such geometric parameter identified by Pearcy,[12] "as the single most important factor in establishing an effective vortex pattern" for the suppression of flow separation is the lateral distance between adjacent vorticies, i.e. spacing angle in the terminology of this paper. However, the spacing angle can not be examined without first understanding the importance of sector angle in vortex generator design, and these parameters are related in this study according to Eq. (6).

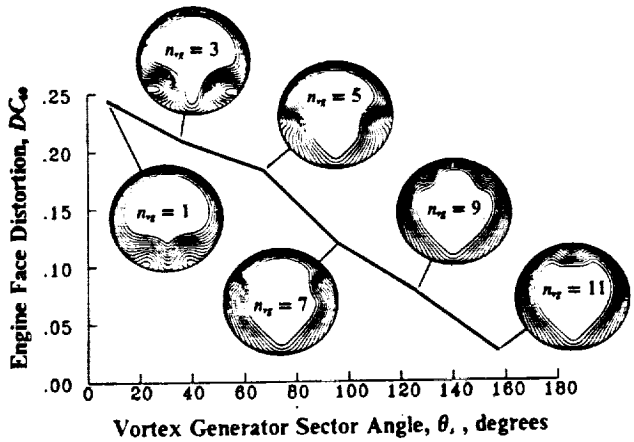

Fig. (15) - Effect of vortex generator sector angle (θ_s) on engine face DC_{60} distortion, VG130 series vortex generators, Test Case 3.2 initial conditions.

Figure 15 presents the effect of generator sector angle θ_s on DC_{60} engine face distortion for the VG130 series generator configurations at the Test Case 3.2 initial conditions. Also shown on Fig. 15 are the engine face recovery maps at each of generator sector angles considered in the analysis. As the number of vortex generator pairs increases, at a constant spacing angle of 15.0°, the sector angle will increase according to Eq. (6). Increasing the number of vortex generators enlarges the sector angle over which the vortex generators are positioned, and this has the effect of 'spreading' the low energy flow more evenly around the the engine face, and consequently decreasing the engine face circumferential distortion. Therefore, improved engine face DC_{60} distortion was achieved by increasing the number of generator pairs installed around the inside periphery of the inlet duct. This can clearly be seen from the engine face recovery maps presented in Fig. 15. The penalty associated with increasing the number of vortex generator pairs is a decrease in engine face total pressure recovery. The computed total pressure loss $\Delta Pt/Pt_0$ associated with an installation composed of eleven (11) generator pairs is 0.008 at the Test Case 3.1 initial conditions and 0.004 at the Test Case 3.2 inlet conditions. These results indicate that the losses associated with vortex generator installations is a strong function of Mach number. In summary, it can be observed that:

The sector angle at which the minimum engine face distortion occurs will be at least 360° although a 'local optimum' can occur depending on the chosen distortion descriptor and angle over which the averaging process takes place.

Presented in Fig. 16 is a comparison between the vortex generator sector angle θ_s characteristics for a generator configuration optimized for the Test Case 3.2 and flight conditions. i.e. VG130 and VG430 series generator configurations respectively. Similar to characteristics found for the generator blade height h/R_t and installation location X_{vg}/R_t, the choice of 'best' sector angle θ_s becomes far more critical under test conditions than flight Reynolds numbers. The sector angle characteristics presented in Fig. 16 also suggests that there is a very limited set of installation geometries where scaling between flight and wind tunnel is even possible, and this is in the neighborhood of a 'best' or optimum sector angle.

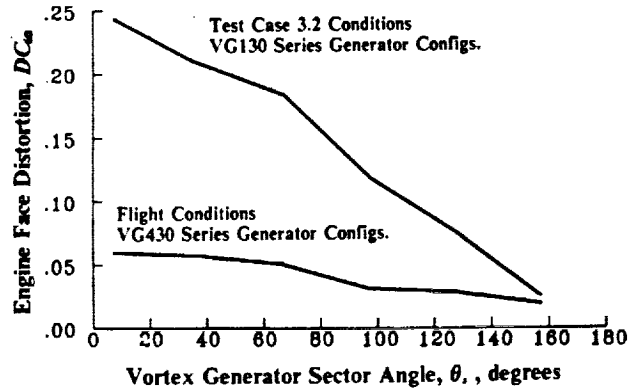

Fig. (16) - Effect of vortex generator sector angle (θ_s) on engine face DC_{60} distortion, VG130 and VG430 series vortex Test Case 3.2 and flight conditions.

Having chosen the 'best' sector angle over which the the vortex generators are placed, the question arises as to what spacing between generator blades will provide the lowest DC_{60} engine face distortion. Figure 17 presents the effect of vortex generator spacing angle α_{vg} on the DC_{60} engine face distortion for a generator installation position at an axial station of 3.0 within the RAE2129 inlet duct operating at the Test Case 3.2 initial conditions. Also shown on Fig. 17 are the individual engine face recovery maps at the spacing angles considered in the analysis. For this sequence, the generator sector angle was held fixed at 157.5°, while the spacing is determined from Eq. (6) for a given number of vortex generators. The spacing of the individual generator blades around the inside periphery of the inlet duct was also determined from Eq. (6). For this set of inlet flow conditions, vortex generator geometry, installation location, and inlet duct aerodynamic characteristics, there existed a generator spacing angle which minimized the DC_{60} engine face circumferential distortion, and this optimum spacing angle was 15.0°.

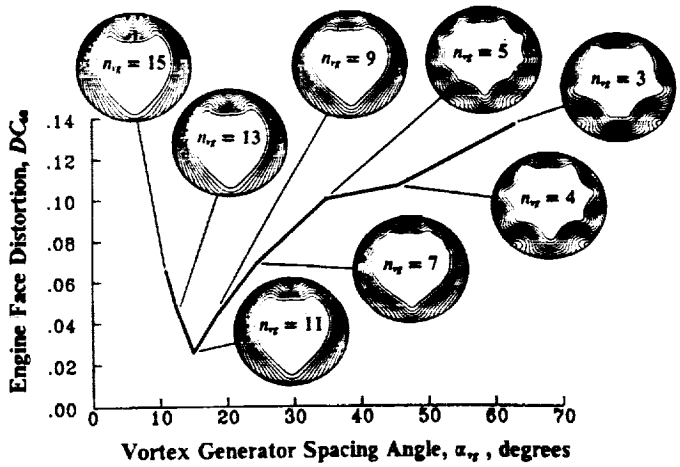

Fig. (17) - Effect of vortex generator spacing angle (α_{vg}) on engine face DC_{60} distortion, VG130 series vortex generators, Test Case 3.2 initial conditions.

This suggests a different design guideline for vortex generator installations from that recommended by Pearcy,[12] but bare in mind that the effectiveness parameter used in that study was retention of the individual vortex identities downstream of the generator blades as measured on a flat plate, while the effectiveness indicator used in this study is the DC_{60} engine face circumferential distortion descriptor. Increasing the vortex generator spacing angle does indeed increase the retention of the individual vortex identities, as can be seen from the series of engine face total pressure recovery maps presented in Fig. 17, but it does not necessarily lead to a minimum DC_{60} engine face distortion. Thus with regards to generator spacing:

For a given configuration of vortex generators positioned at a fixed axial location, there exists a spacing angle which will minimize engine face distortion at a given flow condition.

Presented in Fig. 18 is a comparison between the vortex generator spacing angle α_{vg} characteristics for a generator configuration optimized for both the Test Case 3.2 initial conditions and flight conditions, i.e. VG130 and VG430 series generator configurations respectively. As with the other vortex generator parameters previously discussed, it is apparent that the choice of optimum spacing angle α_{vg} (i.e. lateral distance between generator blades) is a more critical decision for an installation designed for a typical scaled wind tunnel test environment than at flight Reynolds numbers. The spacing angle characteristics presented in Fig. 18 also reveal that there is a very limited set of lateral spacings between generator blades where scaling between flight and wind tunnel is even possible, and these spacing lie in the neighborhood of the optimum angle.

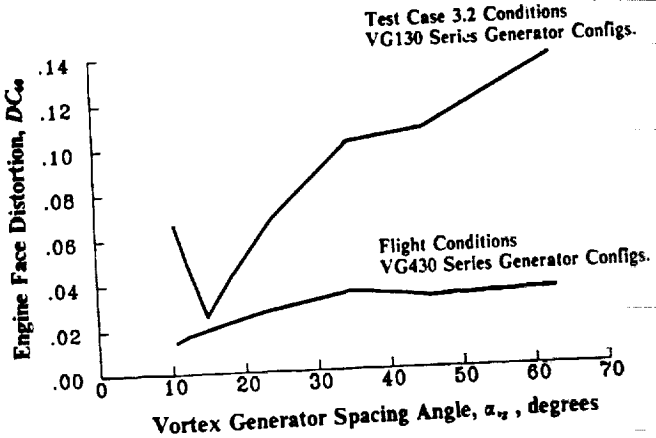

Fig. (18) - Effect of vortex generator spacing angle (α_{vg}) on engine face DC_{60} distortion, VG130 and VG430 series vortex generators, Test Case 3.2 and flight conditions.

Figure 19 presents the effect of vortex generator configuration on DC_{60} engine face distortion as a function inlet throat Mach number M_i, where the total pressure Pt_0 and total temperature Tt_0 were held constant at the Test Case 3.1 values. The vortex generator installations include configurations VG130, VG230, and VG310, which have previously been defined. In general, minimum DC_{60} engine face distortion occurred at the conditions about which the generator installation was optimized. As the flow inlet throat Mach number moves away from the design throat Mach number, the performance of the generator installation degrades, i.e. the DC_{60} engine face distortion increases. The degree to which the performance degrades depends upon the the the geometry, the arrangement, and the placement of the generator installation within the inlet duct. In this example, the 'best' overall performance over the Mach number range from 0.10 to 0.80 was achieved by the VG130 generator installation. The total pressure losses associated with these vortex generator configurations indicate a strong influence of blade height. At the Test Case 3.1 initial conditions, the total pressure losses $\Delta Pt/Pt_0$ were 0.005, 0.008, and 0.010 for configurations VG310, VG130, and VG230 respectively. These configurations correspond to generator blade heights h/R, of 0.060, 0.075, and 0.080.

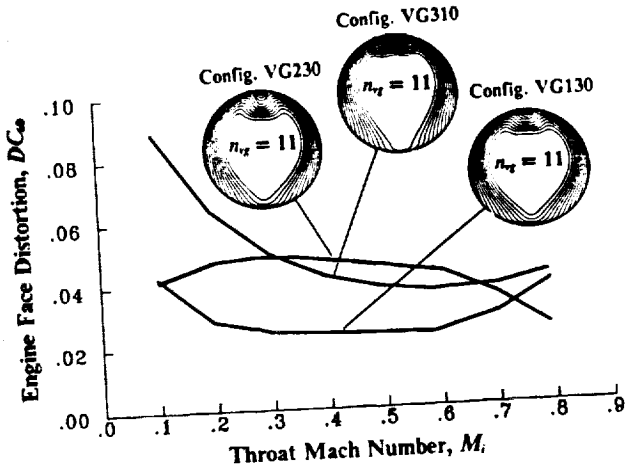

Fig. (19) - Effect of vortex generator configuration on engine face DC_{60} distortion as a function of throat Mach number (M_i), $Pt_0 = 29.889$ in. Hg, $Tt_0 = 293°K$,

A Perspective on Vortex Generator Design

Looking over the experimental work that has been done over the past few years to develop generator installations for inlet ducts, it is quite clear that the purpose of vortex generators for internal flow control is really to limit or minimize engine face distortion, particularly circumferential distortion. Although not explicitly stated as a goal, this is clearly what the development engineers had in mind in the re-engining of the 727-100 center inlet duct for the JT8D series engine.[3] As such, fundamental or even applied research ought to reflect this goal, and make a distinction between suppressing local flow separation (which is the external flow problem), and minimizing engine face distortion (which is the internal flow problem). Suppressing local flow separation is a necessary, but not a sufficient condition in the design of a vortex generator installation for inlet ducts. However, minimizing engine face distortion is both a necessary and sufficient condition for any internal flow management technique. Although these two goals are related, there are many examples where suppressing separation does not lead to a very good engine face distortion.

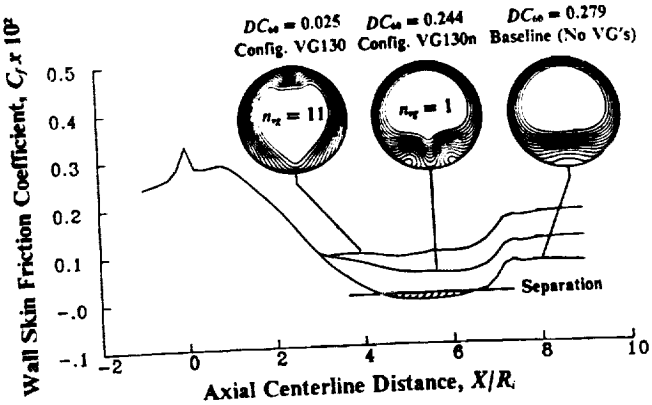

Fig. (20) - Effect of vortex generator configuration on wall skin friction coefficient (C_f) along the $\theta = 180°$ surface element, Test Case 3.2 conditions.

One such example is illustrated in Fig. 20, which presents the wall skin friction coefficient C_f along the the $\theta = 180°$ surface element of the RAE2129 inlet S-duct at the Test Case 3.2 initial conditions for three vortex generator configurations: (1) the baseline configuration, i.e. without vortex generators, (2) vortex generator configuration VG130n, and (3) vortex generator configuration VG130. Vortex generator configuration VG130n has the same geometry, arrangement, and location as configuration VG130, except is has only one (1) pair of co-rotating (or counter-rotating) generators, as compared to eleven (11) pairs of co-rotating generators for configuration VG130. Also shown on Fig. 20 are the DC_{60} engine face distortion values for each of these configurations mentioned, as well as the engine face recovery maps. The baseline inlet duct (i.e. without vortex generators) separates, and this separation is indicated in Fig. 20 as a negative wall skin friction coefficient between the axial centerline stations $X/R_i = 4.5$ and $X/R_i = 6.5$. The computed DC_{60} engine face distortion was 0.279 for the baseline case. With the installation of one (1) co-rotating generator pair, the separation within the RAE2129 inlet duct was eliminated, as indicated by the positive wall skin friction distribution in Fig. 20. But this vortex generator configuration only reduced the the DC_{60} distortion from 0.279 to 0.244. Vortex generator configuration VG130, however also eliminated the flow separation in the RAE2129 inlet S-duct, but it reduced the DC_{60} engine face distortion from 0.279 to 0.025. Thus, the design problem is the control of secondary flow, not the elimination of local flow separation, and the rules for the the design of vortex generator installation and the experimental studies used to understand the aerodynamics of vortex generators must reflect this goal.

Whatever kind of flow management technique is used in inlet ducts, the ultimate goal is to improve the quality of flow entering the engine (this is also true for inlet boundary-layer bleed or blowing). The penalty associated with such flow control can be large, however we can "move the low energy flow around" within the inlet such that it has less of an impact on engine performance. Bare in mind that there is a quantitative measure of the effectiveness of any internal flow management technique, and these are the standard engine distortion descriptors that are unique to each engine company. Therefore, judgements about the effectiveness of any inlet flow technique must be made relative to these descriptors.

Vortex generators are a particularly efficient method of "moving low energy fluid around" so that it has less of an impact on the engine as indicated by the confirmation tests on the 727/JT8D-100 center inlet duct[3] as well as the confirmation experiment conducted on the re-engined 727/TAY651-54 center inlet S-duct[4] At take-off airflow conditions, (i.e. at a throat Mach number of 0.50 and Reynolds number of $12.5x10^6$ based on throat diameter), measurements on the 727/JT8D-100 center inlet S-duct indicate a total pressure loss of 0.002 ($\Delta Pt/Pt_0$) for twenty six (26) generators, while measurements on the 727/TAY651-54 inlet duct indicated a maximum loss of 0.002 ($\Delta Pt/Pt_0$) for thirty two (32) vortex generators. Thus for subsonic flow, vortex generators can be a very low loss method for the management of inlet distortion, particularly at flight Reynolds numbers.

It is important to realize that vortex generators are not being used in vortex flow control to energize the local boundary layer, but rather to build a unique vorticity pattern which interacts with the specific aerodynamic characteristics of the inlet duct such that the engine face distortion remains low over the flight envelope. As such, specific design rules may not exist, but important observations about the aerodynamic properties of vortex flow control can be stated, and these must be tested over time by experimental studies if they are to be incorporated into the design experience.

CONCLUDING REMARKS

The present study demonstrates the capability of the Reduced Navier Stokes RNS3D to design a vortex generator system for the RAE2129 inlet S-duct, where the goal was to minimize inlet distortion by controlling secondary flow. The RAE2129 inlet duct, with the installed vortex generator system, will be tested over a wide range of flow conditions including angle-of-incidence and angle-of-yaw. The experimental data thus generated will be used to validate the present vortex generator model, as well as future models, and will substantiate the concept of vortex flow control and its ability to manage inlet distortion. This research study also established the nature of the performance improvements that can be realized with vortex flow control, and suggests a set of aerodynamic properties (called observations) that can be used to arrive at a successful vortex generator installation design. This study also indicated that scaling between flight and typical wind tunnel test conditions is possible only within a very narrow range of generator configurations close to an optimum installation. This paper also suggests a possible law that can be used to scale generator blade height for experimental testing, but further research in this area is needed before it can be effectively applied to practical problems. Lastly, this study indicated that vortex generator installation design for inlet ducts is more complex than simply satisfying the the requirement of attached flow, it must satisfy the requirement of minimum engine face distortion.

REFERENCES

[1] Advisory Group for Aerospace Research and Development (AGARD), "Engine Response to Distorted Inflow Conditions," AGARD CP-400, Sept., 1986.

[2] Bowditch, D. N. and Coltrin, R. E., "A Survey of Inlet/Engine Distortion Compatability," AIAA Paper No. 83-1166, June 1983.

[3] Kaldschmidt, G., Syltedo, B. E., and Ting, C. T., "727 Airplane Center Duct Inlet Low-Speed Performance Confirmation Model Test for Refanned JT8D Engines - Phase II," NASA CR-134534, Nov. 1973.

[4] Anderson, B.H., Huang, P.S. Paschal, W. A., and Cavatorta, E., "A Study on Vortex Flow Control of Inlet Distortion in The Re-Engined 727-100 Center Inlet Duct Using Computational Fluid Dynamics," AIAA Paper No. 92-0152, 1992.

[5] Briley, W. R. and McDonald, H., "Analysis and Computation of Viscous Subsonic Primary and Secondary Flow," AIAA Paper No. 79-1453.

[6] Briley, W. R., and McDonald, H., "Three-Dimensional Viscous Flows with Large Secondary Velocities," Journal of Fluid Mechanics, March 1984, vol. 144, pp. 47-77.

[7] Levy, R., Briley, W. R., and McDonald, H., "Viscous Primary/Secondary Flow Analysis for Use with Nonorthogonal Coordinate Systems," AIAA Paper No. 83-0556, Jan. 1983.

[8] Anderson, B. H., "The Aerodynamic Characteristics of Vortex Ingestion for the F/A-18 Inlet Duct," AIAA Paper No. 91-0130, Jan. 1991.

[9] Squire, R., "Growth of a Vortex in Turbulent Flow," The Aeronautical Quarterly, Vol. 16, Pt. 3, August 1965, pp 302-306.

[10] Anderson, B. H. and Farokhi, S.,"A Study of Three Dimensional Turbulent Boundary Layer Separation and Vortex Flow Control Using the Reduced Navier Stokes Equations," Turbulent Shear Flow Symposium, Munich, Germany, Sept. 1991.

[11] Willmer, A. C., Brown, T. W., and Goldsmith, E. L., "Effects of Intake Geometry on Circular Pitot Intake Performance at Zero and Low Forward Speeds," Aerodynamics of Power Plant Installation, AGARD CP301, Paper No. 5, 1981.

[12] Pearcy, H. H., "Shock Induced Separation and Its Prevention," in Lachmann, G. V., Boundary Layer and Flow Control, Vol. 2, pp 1166-1355, 1961.

REPORT DOCUMENTATION PAGE

Form Approved
OMB No. 0704-0188

1. AGENCY USE ONLY (*Leave blank*)	2. REPORT DATE	3. REPORT TYPE AND DATES COVERED
	July 1992	Technical Memorandum

4. TITLE AND SUBTITLE

Application of Computational Fluid Dynamics to the Study of Vortex Flow Control for the Management of Inlet Distortion

5. FUNDING NUMBERS

WU-505-62-52

6. AUTHOR(S)

Bernhard H. Anderson and James Gibb

7. PERFORMING ORGANIZATION NAME(S) AND ADDRESS(ES)

National Aeronautics and Space Administration
Lewis Research Center
Cleveland, Ohio 44135-3191

8. PERFORMING ORGANIZATION REPORT NUMBER

E-7039

9. SPONSORING/MONITORING AGENCY NAMES(S) AND ADDRESS(ES)

National Aeronautics and Space Administration
Washington, D.C. 20546-0001

10. SPONSORING/MONITORING AGENCY REPORT NUMBER

NASA TM-105672
AIAA-92-3177

11. SUPPLEMENTARY NOTES

Prepared for the 28th Joint Propulsion Conference and Exhibit cosponsored by the AIAA, SAE, ASME, and ASEE, Nashville, Tennessee, July 6-8, 1992. Bernhard H. Anderson, NASA Lewis Research Center, Cleveland, Ohio and James Gibb, Defense Research Agency, Bedford, England. Responsible person, Bernhard H. Anderson, (216) 433-5822.

12a. DISTRIBUTION/AVAILABILITY STATEMENT

Unclassified - Unlimited
Subject Category 39

12b. DISTRIBUTION CODE

13. ABSTRACT (*Maximum 200 words*)

The present study demonstrates that the Reduced Navier Stokes code RNS3D can be used very effectively to develop a vortex generator installation for the purpose of minimizing the engine face circumferential distortion by controlling the development of secondary flow. The computing times required are small enough that studies such as this are feasible within an analysis-design environment with all its constraints of time and costs. This research study also established the nature of the performance improvements that can be realized with vortex flow control, and suggests a set of aerodynamic properties (called observations) that can be used to arrive at a successful vortex generator installation design. The ultimate aim of this research is to manage inlet distortion by controlling secondary flow through an arrangements of vortex generators configurations tailored to the specific aerodynamic characteristics of the inlet duct. This study also indicated that scaling between flight and typical wind tunnel test conditions is possible only within a very narrow range of generator configurations close to an optimum installation. This paper also suggests a possible law that can be used to scale generator blade height for experimental testing, but further research in this area is needed before it can be effectively applied to practical problems. Lastly, this study indicated that vortex generator installation design for inlet ducts is more complex than simply satisfying the requirement of attached flow, it must satisfy the requirement of minimum engine face distortion.

14. SUBJECT TERMS

Propulsion; Inlets; Computational fluid dynamics

15. NUMBER OF PAGES

12

16. PRICE CODE

A03

17. SECURITY CLASSIFICATION OF REPORT	18. SECURITY CLASSIFICATION OF THIS PAGE	19. SECURITY CLASSIFICATION OF ABSTRACT	20. LIMITATION OF ABSTRACT
Unclassified	Unclassified	Unclassified	